

# Effect of Vanadium and Molybdenum on the Crystallization, Microstructure and Properties of Hypoeutectic Silumin

T. Szymczak \*, G. Gumienny, T. Pacyniak

Department of Materials Engineering and Production Systems, Lodz University of Technology,  
Stefanowskiego 1/15 Street, 90-924 Łódź, Poland

\* Corresponding author. E-mail address: tomasz.szymczak@p.lodz.pl

Received 17.06.2015; accepted in revised form 15.07.2015

## Abstract

The paper presents the results of hypoeutectic silumin 226 grade and silumin produced on its basis through the addition of V and Mo. Vanadium and molybdenum were added as the preliminary alloy AlV10 and AlMo8 in an amount providing the concentration of 0.1; 0.2; 0.3 and 0.4% V and Mo. TDA curves of tested silumins were presented; regardless of the chemical composition there were similar thermal effects. Pressure castings microstructure research revealed the presence in silumins with the addition of V and Mo phases do not occur in silumin without these additives. These phases have a morphology similar to the walled, and their size increases with increasing concentration of V and Mo. The size of the precipitates of these phases silumin containing 0.1% V and Mo does not exceed 10 microns, while 0.4% of the content of these elements increases to about 80 microns. Tests of basic mechanical properties of silumins were carried out. It has been shown that the highest values of tensile strength  $R_m = 295$  MPa and elongation  $A = 4.2\%$  have silumin containing approximately 0.1% V and Mo. Increasing concentrations of these elements causes a gradual lowering of the  $R_m$  and  $A$  values.

**Keywords:** Theory of crystallization, Pressure die-casting, Multi-component silumins, TDA method

## 1. Introduction

In papers [1-9] the results of silumins with additions of Cr, V, W and Mo were presented. Due to the lack of solubility of these elements in aluminum in the solid state in silumins containing them intermetallic phases are formed significantly increasing brittleness of the alloy. In these papers there is no information about the applicability of these elements in silumins for pressure die casting. Taking into account that the process of heat transfer from silumin to pressure casting die is very intense, it may lead to oversaturation solid solutions of these elements. Therefore, in the Department of Materials Technology and Production Systems of Lodz University of Technology silumins to pressure casting with additions of Cr, V, W and Mo are examined.

The aim of this study is to investigate the effect of V and Mo on the crystallization, microstructure and mechanical properties of hypoeutectic 226 silumin designed for pressure die casting.

Figure 1 shows the Al-V phase diagram. Six peritectic transformations occurs on it. As a result of these transformations phases are formed which parameters are shown in Table 1.

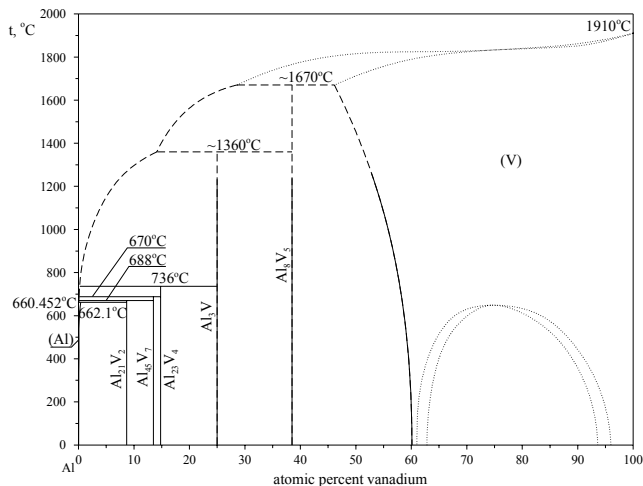


Fig. 1. Aluminium-vanadium phase diagram [10]

Table 1.

The types of phases in the Al-V phase diagram and their crystallographic parameters [10]

Phase	V concentration, wt. %	Pearson symbol	Space group
(Al)	0 do 0.3	<i>cF4</i>	<i>Fm<math>\bar{3}m</math></i>
$Al_{21}V_2$	~8.7 – 9.1	<i>mC104</i>	<i>C2/m</i>
$Al_{45}V_7$	~13.5	<i>mP48</i>	<i>P2</i>
$Al_{23}V_4$	~14.8	<i>mP180</i>	<i>P2/m</i>
$Al_3V$	~25	<i>aP30</i>	<i>P<math>\bar{1}</math></i>
$Al_8V_5$	39.5	<i>cI52</i>	<i>I<math>\bar{4}3m</math></i>
(V)	~46 – 100	<i>cI2</i>	...
$AlV_3$	~75	<i>cP8</i>	<i>R<math>\bar{3}m</math></i>
$\beta AlV_3$	~75	<i>h**</i>	...
$\alpha AlV_3$	~75	<i>t**</i>	...

The solubility of vanadium in aluminum is negligible and amounts to maximum 0.6 wt. % (~ 0.2 at. %). The maximum solubility of aluminum in vanadium is 54 wt. % at a temperature of about 1670°C. From the data presented in Fig. 1 it follows that even a slight addition of vanadium raises the temperature of solidification of Al-V alloy.

Al-Mo phase diagram is presented in papers [11, 12]. From the data presented in it results the lack of solubility of Mo in Al as was in the case of vanadium. The maximum solubility of Al in Mo is 20% at the temperature of ~2150°C. The phases occurring in the this diagram crystallize mainly due to peritectic transformations. These include phases:  $Al_{12}Mo$ ,  $\beta Al_5Mo$ ,  $\alpha Al_5Mo$ ,  $Al_{22}Mo_5$ ,  $Al_{17}Mo_4$ ,  $Al_4Mo$ ,  $Al_3Mo$ ,  $Al_{63}Mo_{37}$ ,  $AlMo$  and  $AlMo_3$ . Apart from them, in this arrangement, there is another phase ( $Al_8Mo_3$ ) formed from a liquid at a temperature of 1546°C (congruent point at Mo concentration of about 27.3 at. %). Molybdenum just as vanadium raises the crystallization temperature of aluminum alloys.

In paper [13] the Mo-V phase diagram was presented. It follows that Mo and V create a solid solution with unlimited solubility in the solid state.

## 2. Methodology of the research

The preparation of the liquid silumin and tested castings were performed under the production conditions of the Innovation and Implementation Enterprise Wifama-Prexer Ltd., Poland.

To the study 226 silumin was used. This is a typical hypoeutectic silumin to pressure die casting. Silumin was melted in a gas shaft furnace with a capacity of 1.5 tons. The chemical composition of 226 silumin is presented in Table 2.

Table 2.

The chemical composition of 226 silumin

Chemical composition, wt. %							
Si	Cu	Zn	Fe	Mg	Mn	Ni	Al
8,74	2,42	0,97	0,88	0,34	0,23	0,11	reszta

Silumin was refining within the shaft furnace with use of solid refiner Ecosal Al 113.S. After smelting and refining silumin was deslagged and transported to the holding furnace set near to pressure machine. In the holding furnace to silumin master alloys AlV10 and AlMo8 were added in a quantity such that the concentration of additives in individual melts of at approximately 0.1; 0.2; 0.3 and 0.4% V and Mo. Studies were also carried out for 226 alloy which not contain these additives (chemical composition complies with the Tab. 2). For each variant of chemical composition the housing roller blinds castings were made with predominant wall thickness of 2 mm. Castings were made with using pressure machine with a horizontal cold chamber Idra 700S. Thermal and derivative analysis (TDA) silumin was used to examination of the crystallization process. The TDA method have been used to study the alloys: iron, aluminum, bronze, magnesium and cobalt [14-17].

For recording TDA curves of silumin PtRh10-Pt thermocouple placed in the sampler TDA10m-TUL was used [18]. The temperature of silumin poured into the sampler stemmed from the temperature inside the holding furnace (750°C).

The strength tests were carried out on specimens cut from pressure castings of housing. For each tested chemical composition of silumin three specimens were cut from one casting. They had a rectangular cross section with dimensions of 2/10 mm as recommended by the standard [19]. Tensile tests were performed on a Instron 3382 machine using a speed of 1 mm/min. During the tensile tests were determined: tensile strength  $R_m$ , yield strength  $R_{p0.2}$  and elongation A.

HB hardness tests were performed on Briviskop HPO-2400. We used a ball with a diameter of  $d = 2.5$  mm and a load of 613 N.

Silumin microstructure was investigated on samples taken from pressure castings. Metallographic specimens were etched with 2% aqueous solution of HF and tested at a magnification of  $\times 1000$  on metallurgical microscope Nikon Eclipse MA200.

## 3. Results

Figure 2 shows the TDA curves of 226 silumin. The crystallization process of this silumin was presented in [12, 18].

There are three thermal effects on the derivative curve, which correspond to a crystallization of the following phases: solid solution  $\alpha$  (AB effect), triple eutectic  $\alpha + \text{Al}_9\text{Fe}_3\text{Si}_2 + \beta$  (BCDEH effect) and quadruple eutectic  $\alpha + \text{Al}_2\text{Cu} + \text{AlSiFeCuMgMnNi} + \beta$  (HKL effect). Placing to the silumin V and Mo additives, regardless of their concentration resulted in occurrence on the derivative curve analogous thermal effects in comparison to the silumin without these additives (Fig. 2). The representative TDA curves for silumin with the addition of V and Mo are shown in Figure 3. The curves were plotted for silumin with the highest concentration of V and Mo (0.4 wt. %).

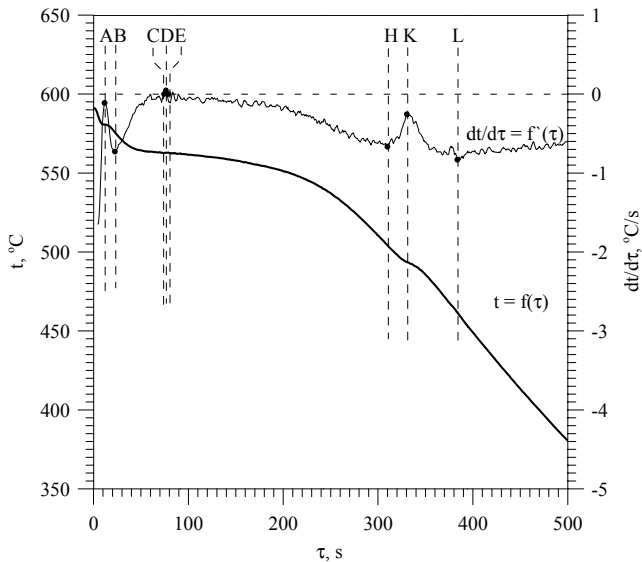


Fig. 2. The representative TDA curves of 226 silumin

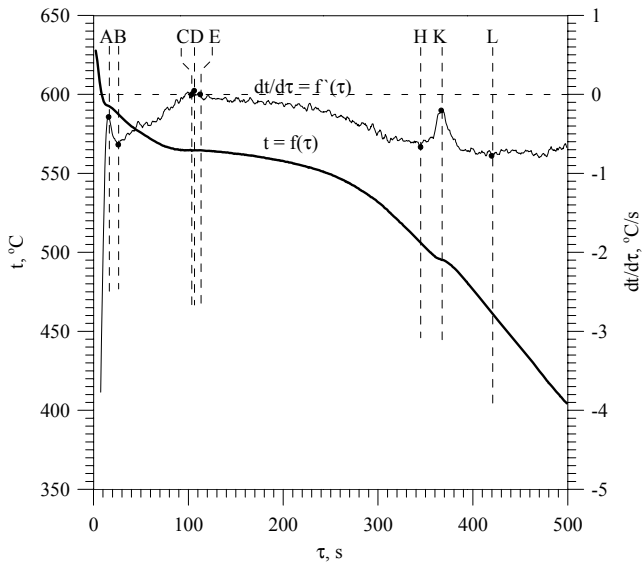


Fig. 3. The representative TDA curves of silumin with an addition of about 0.4 wt. % V and Mo

Lack of solubility V and Mo in the phase  $\alpha$  and nonoccurrence of additional thermal effects on TDA curves may indicate that these elements are located in quadruple eutectic

crystallized from the remaining liquid. Accordingly, after addition of V and Mo it should be as follows:  $\alpha + \text{Al}_2\text{Cu} + \text{AlSiFeCuMgMnNiV} + \beta$ . Table 3 (a, b) shows a setting-up of the temperature and cooling rate at the characteristic points for the basic silumin and with the addition of V and Mo.

Table 3 (a, b).

The setting-up of the temperature (a) and cooling rate (b) at the characteristic points for the basic silumin and with the addition of 0.1–0.4 wt. % V and Mo.

a)

V and Mo concentration, wt. %	Temperature t, °C							
	A	B	C	D	E	H	K	L
0.0	581	576	563	563	563	504	494	462
0.1	585	580	564	564	564	507	495	454
0.2	587	583	-	564	-	504	495	464
0.3	590	585	566	566	566	506	497	461
0.4	593	587	564	565	565	506	495	462

b)

V and Mo concentration, wt. %	dt/dτ, °C/s							
	A	B	C	D	E	H	K	L
0.0	-0.11	-0.73	0.01	0.05	-0.01	-0.67	-0.26	-0.83
0.1	-0.48	-0.71	0.02	0.04	0.00	-0.68	-0.22	-0.79
0.2	-0.18	-0.76	-	-0.01	-	-0.64	-0.23	-0.79
0.3	-0.29	-0.79	-0.03	0.02	-0.03	-0.60	-0.21	-0.76
0.4	-0.29	-0.64	-0.04	0.05	-0.01	-0.67	-0.20	-0.78

According to the data in the Tab. 3a results the temperature increase at points A and B with increasing concentrations of V and Mo. Therefore, these additives increase the temperature of primary  $\alpha$  phase crystallization. This is consistent with the Al-V and Al-Mo phase diagrams. There was no clear effect of V and Mo at the temperature in the other characteristic points and the cooling rate dt/dτ [Tab. 3(a, b)].

Figure 4 shows the microstructure of 226 silumin pressure die cast.

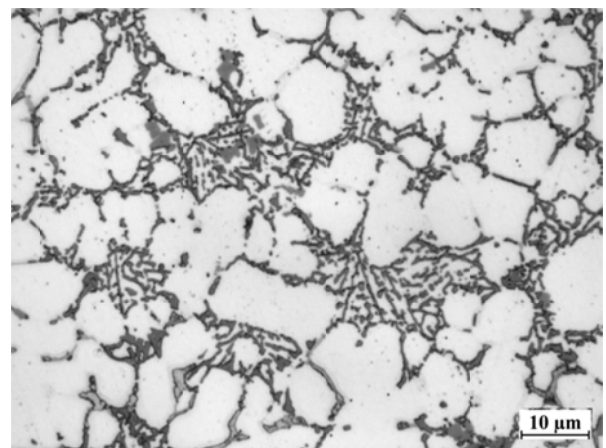


Fig. 4. The microstructure of 226 silumin obtained in the pressure die casting:  $\alpha$ ,  $\alpha + \text{Al}_9\text{Fe}_3\text{Si}_2 + \beta$ ,  $\alpha + \text{Al}_2\text{Cu} + \text{AlSiFeCuMgMnNi} + \beta$

The presented microstructure (Fig. 4) consists of  $\alpha$  dendrites and eutectic mixtures: triple  $\alpha + \text{Al}_9\text{Fe}_3\text{Si}_2 + \beta$  and quadruple  $\alpha + \text{Al}_2\text{Cu} + \text{AlSiCuFeMgMnNi} + \beta$ . This microstructure corresponds to the crystallization process shown in TDA curves (Fig. 2). The components of this microstructure due to the high rate of heat transfer through the mold are characterized by high fragmentation. The microstructure of pressure die castings made of silumin containing V and Mo at about 0.1, 0.2, 0.3 and 0.4 wt. % is shown in Figure 5 (a-d). Regardless of V and Mo concentration in the microstructure of the tested silumin there were, as it was in a "pure" 226 silumin, dendrites of  $\alpha$  phase, triple eutectic  $\alpha + \alpha \text{Al}_9\text{Fe}_3\text{Si}_2 + \beta$  and quadruple eutectic, in which additionally there were V and Mo atoms -  $\alpha + \text{Al}_2\text{Cu} + \text{AlSiCuFeMgMnNiVMo} + \beta$ .

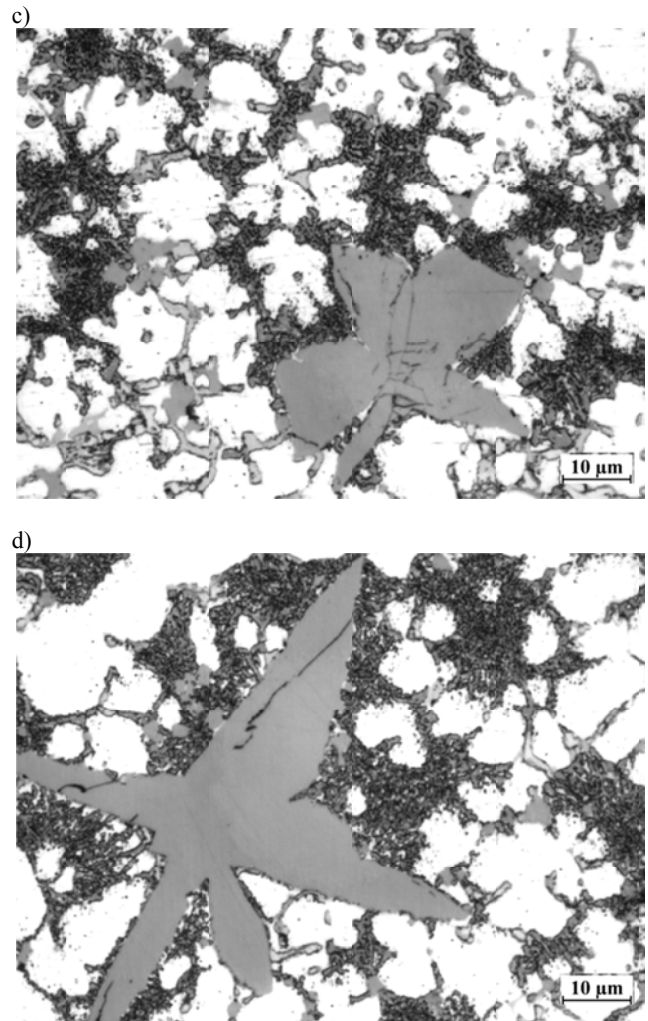
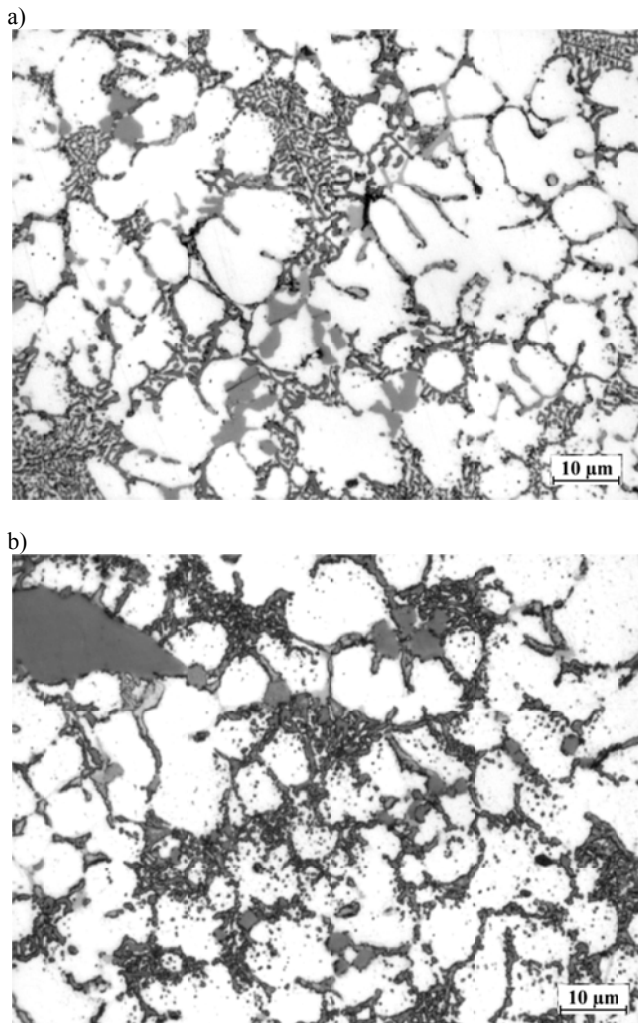


Fig. 5 (a-d). The microstructure of pressure die cast made of the tested silumin with the addition of V and Mo approximately: a – 0.1%, b – 0.2%, c – 0.3%, d – 0.4%:  $\alpha$ ,  $\alpha + \text{Al}_9\text{Fe}_3\text{Si}_2 + \beta$ ,  $\alpha + \text{Al}_2\text{Cu} + \text{AlSiCuFeMgMnNiVMo} + \beta$

Furthermore, in the microstructure of silumin containing V and Mo there are phases with morphology similar to walled which did not occur in 226 silumin without these elements. In silumin containing of about 0.1% V and Mo, these phases are relatively small (Fig. 5a). Their biggest sizes do not exceed 10 microns. Increasing the concentration of V and Mo increases the size of walled phases. In silumin containing the highest concentration of V and Mo (approximately 0.4 wt. %) the dimensions of these phases reach up to about 80 microns (Fig. 5d). Such a big precipitations in the pressure die casting of ~2 mm wall thickness may indicate start of silumin crystallization before introducing it into the mould. Increasing the crystallization temperature due to the addition of V and Mo and relatively low holding temperature in the holding furnace (resulting from requirements for pressure casting technology) and may cause phases crystallization in a shank ladle or inside the pressure chamber. The lack of additional thermal effect on the TDA curves of silumin with V

and Mo (Fig. 3) is caused probably by too low temperature of alloy poured into the sampler.

In Table 4 and in Figure 6 (a-c) the results of testing the mechanical properties of the basic silumin and silumin containing 0.1 ÷ 0.4% V and Mo were presented.

Table 4.

The mechanical properties of the tested silumin without and with the addition of V and Mo

V and Mo concentration, wt. %	Mechanical properties			
	$R_m$ , MPa	$R_{p0,2}$ , MPa	A, %	HB
0.0	251	120	3,7	120
0.1	295	118	4,2	120
0.2	261	124	4,0	112
0.3	223	126	2,9	107
0.4	212	122	2,7	114

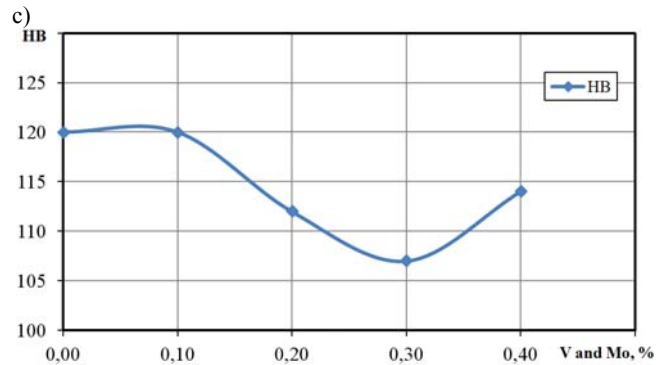
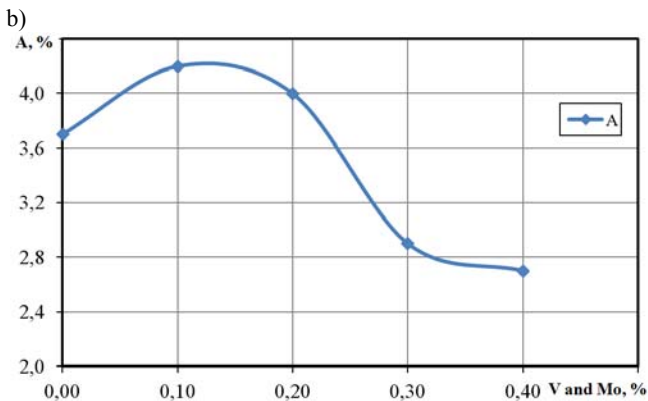
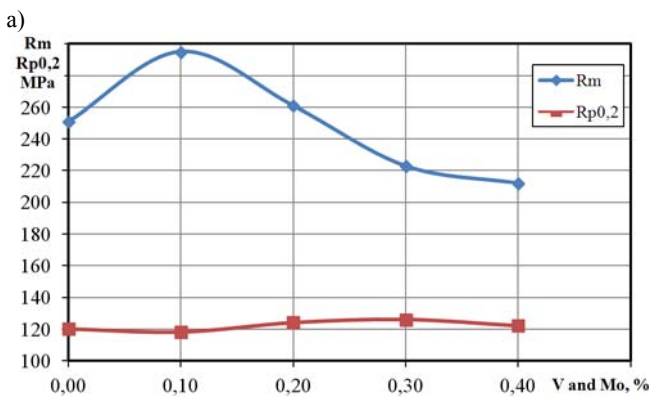


Fig. 6 (a-c). The mechanical properties of 226 silumin without and with the addition of V and Mo

The presented data show that 226 silumin has a tensile strength 251 MPa; yield strength 120 MPa; A relative elongation 3.7% and a hardness 120 HB. An addition of 0.1 wt. % V and Mo has increased tensile strength to 295 MPa and elongation to 4.2%. This gives a relative increase of  $R_m$  by 17.5% and A by 13.5%. Further increasing the concentration of V and Mo in silumin resulted in a gradual reduction of its  $R_m$  and A. The lowest values of  $R_m = 212$  MPa and  $A = 2.7\%$  were obtained for silumin with the highest concentration of V and Mo (approximately 0.4%). However, changes in these parameters vs the concentration of V and Mo have been inconclusive. The highest value of  $R_{p0,2} = 126$  MPa was obtained at a concentration of V and Mo approximately 0.3%, and hardness was the largest in the alloy without V and Mo and at the concentration of 0.1%. The presented data show that the highest values of  $R_m$  and A were obtained in silumins where walled phases have small dimensions. The increase in the phases size taking place with increasing concentrations of V and Mo reduces  $R_m$  and A. It can be assumed that the strengthening of silumin is not the result of the existence the intermetallic phases but by the supersaturation of solid solutions of vanadium and molybdenum.

## 4. Summary

From the data included in this paper we can draw the following conclusions:

- on the TDA curves of all tested silumins, there are three thermal effects derived from the crystallization successively:  $\alpha$  (Al) phase and the eutectic mixture: triple and quadruple,
- in the silumin microstructure after the addition of V and Mo phases with morphology similar to the walled crystallize; they do not occur in the "pure" silumin 226. Their size increases with increasing concentrations of V and Mo,
- the highest values of mechanical properties were as follows:  $R_m = 295$  MPa for 0.1% V and Mo,  $A = 4.2\%$  also for 0.1% V and Mo,  $R_{p0,2} = 126$  MPa for 0.3% and  $HB = 120$  at a concentration of 0.0 and 0.1% V and Mo,
- there is the possibility of increasing  $R_m$  and A of pressure die castings made of silumin with V and Mo by supersaturation of solid solutions occur in the microstructure.

## Acknowledgements

Project financed from means of the National Centre for Research and Development in years 2013 ÷ 2015 as project UDA-POIG.01.04.00-10-079/12.

## References

- [1] Pietrowski, S. (2001). *Silumins*. Łódź. Publishing house of Lodz University of Technology.
- [2] Binczyk, F. & Piątkowski, J. (2003). Crystallization silumin AlSi17 containing Cr, Co and Ti. *Archives of Foundry*. 3(9), 39-44. (in Polish).
- [3] Sahoo, K.L. & Pathak, B.N. (2009). Solidification behaviour, microstructure and mechanical properties of high Fe-containing Al-Si-V alloys. *Journal of Materials Processing Technology*. 209, 798-804.
- [4] Sahoo, K.L., Das, S.K. & Murty B.S. (2003). Formation of novel microstructures in conventionally cast Al-Fe-V-Si alloys. *Materials Science and Engineering*. 355(1-2), 193-200.
- [5] Pietrowski, S., Władysiak, R. & Pisarek, B. (1999). Crystallization, structure and properties of silumins with cobalt, chromium, molybdenum and tungsten admixtures. In International Conference Light Alloys and Composites, 13-16 May 1999 (77-83).
- [6] Pietrowski, S., Władysiak, R. & Pisarek, B. (1998). Eutectic silumin with an additions of Cr, Mo, W, and Co. *Solidification of Metals and Alloys*. 13, 103-108.
- [7] Pietrowski, S. & Szymczak, T. (2009). Silumins alloy crystallization. *Archives of Foundry Engineering*. 9(3), 143-158.
- [8] Pietrowski, S., Szymczak, T., Siemińska-Jankowska, B. & Jankowski, A. (2010). Selected characteristic of silumins with additives of Ni, Cu, Cr, Mo, W and V. *Archives of Foundry Engineering*. 10(2), 107-126.
- [9] Pietrowski, S. & Szymczak, T. (2010). Modification of silumins with an alloying elements. In S. Pietrowski (Eds.), *Tendencies of Optimization of the Production System in Foundries*. (pp. 277-290). Katowice-Gliwice: Polish Academy of Sciences, Foundry Commission. (in Polish).
- [10] Alloy Phase Diagrams. ASM Handbook Vol. 3. 1992.
- [11] Okamoto, H. (2010). Al-Mo (Aluminum-Molybdenum). *Journal of Phase Equilibria and Diffusion*. 31(5), 492-493.
- [12] Szymczak, T., Gumienny, G., Walas, K. & Pacyniak, T. (2015). Effect of Tungsten and Molybdenum on the Crystallization, Microstructure and Properties of Silumin 226. *Archives of Foundry Engineering*. 15(3), 61-66.
- [13] Zheng, F., Argent, B.B. & Smith, J.F. (1999). Thermodynamic Computation of the Mo-V Binary Phase Diagram. *Journal of Phase Equilibria*. 20(4), 370-372.
- [14] Pietrowski, S., Pisarek, B., Władysiak, R., Gumienny, G. & Szymczak, T. (2009). TDA curves of metals alloys and the control of their quality. In Szajnar J. *Advances In Theory and Practice Foundry*, (pp. 345-377), Katowice – Gliwice, PAN. (in Polish).
- [15] Pisarek, B.P. (2013). Model of Cu-Al-Fe-Ni Bronze Crystallization. *Archives of Foundry Engineering*. 13(3), 72-79.
- [16] Rapiejko, C., Pisarek, B., Czekaj, E. & Pacyniak, T. (2014). Analysis of the Crystallization of AZ91 Alloy by Thermal and Derivative Analysis Method Intensively Cooled in Ceramic Shell. *Archives of Foundry Engineering*. 14(1), 97-102.
- [17] Kacprzyk, B., Szymczak, T., Gumienny, G. & Klimek, L. (2013). Effect of the Remelting on Transformations in Co-Cr-Mo Prosthetics Alloy. *Archives of Foundry Engineering*. 13(3), 47-50.
- [18] Szymczak, T., Gumienny, G. & Pacyniak, T. (2015). Effect of tungsten crystallization process, the microstructure and properties of silumin 226. *Innowacje w odlewnictwie ciśnieniowym 2015*. Kraków: The Transactions of the Foundry Research Institute. (in Polish).
- [19] PN-EN 1706:2011. Aluminum and aluminum alloys. Castings. The chemical composition and mechanical properties. (in Polish).